CircMBOAT2 promotes FASN-mediated lipid metabolism reprogramming and progression in intrahepatic cholangiocarcinoma

Xiaopeng Yu
Department of General Surgery, Xinhua Hospital, Shanghai Jiao Tong University School of Medicine, Shanghai 200092, China

Huanjun Tong
Department of General Surgery, Xinhua Hospital, Shanghai Jiao Tong University School of Medicine, Shanghai 200092, China

Jialu Chen
Department of General Surgery, Xinhua Hospital, Shanghai Jiao Tong University School of Medicine, Shanghai 200092, China

Chenwei Tang
Department of General Surgery, Xinhua Hospital, Shanghai Jiao Tong University School of Medicine, Shanghai 200092, China

Shuqing Wang
Department of General Surgery, Xinhua Hospital, Shanghai Jiao Tong University School of Medicine, Shanghai 200092, China

Yu Si
Department of Blood Transfusion, Xinhua Hospital, Shanghai Jiao Tong University School of Medicine, Shanghai 200092, China

Shouhua Wang
Department of General Surgery, Xinhua Hospital, Shanghai Jiao Tong University School of Medicine, Shanghai 200092, China

Zhaohui Tang (✉ tangzhaohui@xinhuamed.com.cn)
Department of General Surgery, Xinhua Hospital, Shanghai Jiao Tong University School of Medicine, Shanghai 200092, China

---

Research Article

Keywords: Intrahepatic cholangiocarcinoma, circMBOAT2, PTBP1, FASN, Lipid metabolism

Posted Date: May 2nd, 2022

DOI: https://doi.org/10.21203/rs.3.rs-1525828/v2

Abstract

Background

The carcinogenic role of FASN by regulating lipid metabolism reprogramming has been well established in multiple tumors. However, whether mechanisms during intrahepatic cholangiocarcinoma (ICC) progression such as circRNAs regulate FASN expression remains unknown.

Methods

Five paired ICC and adjacent normal tissues were used to screen the lipid metabolism-associated differentially expressed circRNAs by high-throughput RNA sequencing; the biological role of circMBOAT2 was determined by gain or loss of function experiments. Fluorescence in situ hybridization (FISH), RNA immunoprecipitation (RIP) and RNA pull-down assays were used to analyze the interaction of circMBOAT2 with PTBP1 and PTBP1 with FASN. Coimmunoprecipitation (co-IP) was used to investigate the ubiquitin binding of PTBP1. Non-targeted lipidomics was applied to detect changes in metabolite composition.

Results

CircMBOAT2 (has_circ_0007334 in circBase) was frequently upregulated in ICC tissues and correlated with tumor size. Knockdown circMBOAT2 inhibits proliferation of ICC cells. Mechanistically, circMBOAT2 combines with PTBP1 and protect PTBP1 from ubiquitin/proteasome-dependent degradation, impairing the function of PTBP1 to transfer FASN mRNA from the nucleus to the cytoplasm. Moreover, circMBOAT2 and FASN have the same effect on fatty acid profile, unsaturated fatty acids instead of saturated fatty acids are primarily regulated and associated with malignant behaviors of ICC cells.

Conclusions

Our results identified that circMBOAT2 stabilized PTBP1 and facilitated ICC lipid metabolic reprogramming via the modulation of FASN mRNA cytoplasmic export, suggesting that circMBOAT2 may serve as an available therapeutic target for ICC with active lipid metabolism.

Background

Intrahepatic cholangiocarcinoma (ICC) accounts for 8–10% of biliary tract cancer (BTC) and 10–15% of primary liver cancer[1], including mass-forming (MF) type, periductal infiltrating (PI) type, and intraductal growth (IG) type[2]. The incidence of ICC has been increasing globally in the past two decades[3,4]. Due to its highly aggressive and malignant biologic behavior, as well as the lack of effective treatments, ICC has an

extremely poor prognosis, especially for advanced stage patients[4]. This poor long-term survival outlook highlights further improvements in disease control by understanding the mechanisms of ICC. Although many previous reports have documented abundant molecular anomalies, in either coding or non-coding RNAs[5,6], are involved and play important roles in the pathogenic process of ICC, the precise molecular mechanisms are still largely unclear.

Circular RNAs (circRNAs) compromise a class of regulatory RNAs with covalently closed single-stranded loop conformation produced from direct backsplicing or exon skipping of precursor mRNA[7]. Dysregulation of circRNAs expression has been found in different pathological processes including the pathogenesis of breast[8], liver[9], lung[10], and esophagus[11] cancers. In the past, circRNAs were considered to be a by-product of splicing errors with little function[12]. Whereas, several circRNAs functions such as miRNA sponges[8,13], protein scaffold[10,14], and even as protein translation templates[5,15] were found over the years. These foundations suggest that circRNAs play functional roles in biological processes and act as potential clinical molecular markers. As a consequence, provide new insights into the treatment of cancer and other human diseases.

Tumor cells live in an environment of hypoxia and relative lack of nutrients. In order to meet the needs of cells for energy and their own biosynthetic materials during rapid tumor growth, their metabolic pattern changes, which is called metabolic reprogramming[16]. Metabolic reprogramming is one of the hallmarks of malignant tumors[17], no exception for intrahepatic cholangiocarcinoma. ICC was characteristic of lactic dehydrogenase (IDH) mutation, which was found in nearly 20% of ICC patients by whole-exome sequencing[18]. Hexokinase (HK), a key enzyme catalyzes glucose to glucose-6-phosphate, was abnormally elevated in ICC associated with liver fluke and associated with poor prognosis[19]. However, mechanism of metabolic reprogramming in these papers mainly focuses on glycometabolism. Further insight into the role and mechanism of lipid metabolism reprogramming in ICC may be helpful to understand the development and progression of ICC deeply. Fatty acid synthase (FASN) is the key enzyme for fatty acid synthesis. It has been reported that FASN plays a dominant role in amounts of tumors such as breast[20], ovary[21], liver[22], and colorectum[23] cancers. High expression of FASN was significantly correlated with the advanced stage in cholangiocarcinoma patients[24]. Knockdown of FASN inhibits ICC cell proliferation and invasion[24], however, mechanism regulating FASN expression and function in ICC and the changes of metabolic profile regulated by FASN are still unclear.

In the present study, we demonstrate that a specific circRNA associated with lipid metabolic reprogramming, circMBOAT2 (has_circ_0007334 in circBase), mapping to the chromosome 2p25 amplicon in ICC, is frequently upregulated in ICC patients and predicts poor survival. We further reveal that circMBOAT2 could bind with polypyrimidine tract binding protein 1 (PTBP1), a sort of ribosomal protein never been reported in ICC. This protects PTBP1 from being degraded in a ubiquitination-dependent manner. PTBP1, as a sort of ribosomal protein, could bind and export FASN mRNA to the cytoplasm sequentially, as a result of which, FASN was highly translated. Lipidomics indicate that circMBOAT2 and FASN have the same effect on fatty acid level, unsaturated fatty acids instead of

saturated fatty acids are primarily regulated by them. Our data suggest that circMBOAT2 may exert as a potential therapeutic target against ICC.

Methods

Patients and tissue

This study has been approved by the Ethics Committee of Xinhua Hospital (Shanghai, China), and the study was informed in accordance with Declaration of Helsinki. Written informed consent was obtained from the patients before the study began.

Tumor tissues and adjacent normal tissues were obtained from 26 patients underwent radical resection between 2015 and 2017 at Xinhua hospital. Each tissue sample was snap-frozen in liquid nitrogen for further analysis. All of the patients in this study belonged to the same ethnic group. The patients were selected according to the criteria: (1) All clinicopathological diagnoses were confirmed by two pathologists. (2) None of the patients received any treatments before surgery. (4) Availability of complete follow-up data and not lost follow-up. (5) No death in the perioperative period. (6) No history of other synchronous malignancies.

RNA sequencing

Total RNA from tissues and cells were isolated using Hipure Total RNA Mini Kit (Magen) according to the protocol. RNAs were eluted with 50μl of RNase-free water and then re-purified the concentration and integrity of the extracted total RNA was estimated by Qubit 3.0 Fluorometer (Invitrogen, Carlsbad, California), and Agilent 2100 Bioanalyzer (Applied Biosystems, Carlsbad, CA), respectively. RNA samples with a RIN value of at least 7.0 or higher was used for further processing. RNA-seq library was prepared with approximately 1μg of total RNA using KAPA Stranded RNA-Seq Kit with RiboErase (HMR) for Illumina Platforms (Kapa Biosystems, Inc., Woburn, MA). Briefly, ribosomal RNA was removed from total RNA. Next, first strand and directional second strand synthesis were performed. Then the A tailing and adapter ligation were performed with the purified cDNA. Finally, the purified, adapter-ligated DNA was amplified. The library quality and concentration was assessed by utilizing a DNA 1000 chip on an Agilent 2100 Bioanalyzer. Accurate quantification for sequencing applications was determined using the qPCR-based KAPA Biosystems Library Quantification kit (Kapa Biosystems, Inc., Woburn, MA). Each library was diluted to a final concentration of 10 nM and pooled equimolar prior to clustering. Paired-End (PE) sequencing was performed on all samples. For circRNA expression analysis, the read was to mapped genome using the STAR and DCC was used to identify the circRNAs and to estimate the circRNAs expression. TMM (trimmed mean of M-values) was used to normalize the gene expression. Differentially expressed genes were identified using the edgeR program.

Cell cultures

Human cholangiocarcinoma cell lines (RBE, HCCC-9810 and QBC-939), and human normal bile duct epithelium cell line (H69) were obtained from the Cell Bank of the Shanghai Cell Bank of the Chinese Academy of Sciences (Shanghai, China). Cells were maintained at 37℃ in a 5% CO_2 humidified incubator, and cultured in RPMI-1640 (Gibco) (RBE and QBC-939) or DMEM (Gibco) (HCCC-9810) supplemented with 10% fetal bovine serum (Gibco) and 1% antibiotics(Gibco). Cells have not been in culture for longer than 2 months.

RNAi and plasmid construction

SiRNAs duplexes were synthesized by GenePharma (Suzhou, China) and transfected into cells using lipofectamine 2000 (Invitrogen) according to the manufacturer's protocol. Lentivirus for knockdown of circMBOAT2 and plasmid for circMBOAT2 overexpression were obtained from GeneChem (shanghai, China). The target sequences for constructing lentiviral shRNAs and siRNAs are listed in Additional file 2.

RNA extraction and qRT-PCR analysis

Total RNA derived from ICC tissues and cells was extracted using TRIzol reagent (TaKaRa, Dalian, China) according to the manufacturer's instructions. RNA was reverse transcribed into cDNA using a Primer-Script one step RT-PCR kit (TaKaRa, Dalian, China). Hieff UNICON® qPCR SYBR® Green Master Mix (Yeasen, Shanghai, China) was used for qRT-PCR. The circRNA and mRNA levels were normalized by GAPDH, β-actin or U3. The fold change in relative expression of RNAs was calculated using the $2^{-\Delta\Delta Ct}$ methods. Oligonucleotides sequences are listed in Additional file 2.

RNase R treatment

Two micrograms of total RNA was incubated 30 min at 37 °C in the absence or presence of 5 U/μg RNase R (Geneseed, Guangzhou, China) and the resulting RNA was subsequently purified by RNeasy Mini Kit (Qiagen, Germany), and then analyzed by qRT-PCR.

RNA fluorescence in situ hybridization (FISH)

Oligonucleotide-modified probe sequence for circMBOAT2 and FASN was synthesized from Sangon Biotech (Shanghai, China). Fixed cells were washed in PBS. The cell suspension was pipetted onto autoclaved glass slides, followed by dehydration with 70, 80 and 100% ethanol. Then hybridization was performed at 37 °C overnight in a dark moist chamber. After being washed twice in 50% formamide/2 × SSC for 5 min, the slices were incubated with the regents in Alexa FluorTM 488 Tyramide SuperBoost™ Kits (Thermo Fisher Scientific, Waltham, USA) for 30 min and sealed with parafilm containing DAPI. The images were acquired using a fluorescence microscopy (OLYMPUS, Japan). The probe sequences were shown as below:

circMBOAT2: 5'- Cy3- CACTACAAAGTTGACTTGTGCATGTTCTCCACT- 3'

FASN: 5'- digoxin- GCGTAGGATGGAATCTCGGAAGCGGTC- 3'

In vitro cell phenotypic assays

For CCK-8 proliferation assay, 2×10^3 cells were seeded in 100 μl complete culture media in 96-well plates for various time periods. Cell Counting Kit-8 assay was performed to measure cell viability according to the manufacturer's instructions. For 5-Ethynyl-2'-deoxyuridine (EdU) proliferation assay, BeyoClick^{TM} EdU proliferation assay (Beyotime, Shanghai, China) was used according to the manufacturer's protocol. For migration assays, transwell filter champers (8-μm pore size, Corning, NY) were used according to the manufacturer's instructions. Cells migrated through the membrane were fixed by 4% paraformaldehyde, stained with 0.1% crystal violet, and counted under a light microscope. Cells were incubated with 10μM EdU for two hours, stained with DAB then visualized under a light microscope. For scratch experiment, cells were plated into a six-well plate after 48-hours transfection then scratched by pipette tip. After 24-hours incubation with serum-free medium, the wound width was checked.

Flow cytometric analysis

For cell cycle analysis, after 48 h of incubation, transfected ICC cells were washed with cold phosphate-buffered saline (PBS) and incubated in ice-cold 70% ethanol at 4 °C overnight. Then, cells were incubated with propidium iodide for 30 min and analyzed for cell cycle distribution using a flow cytometer (FACS Calibur, BD Biosciences, USA). Data were analyzed by FlowJo 10.6.2 software and presented as the percentage of cell phase distribution including G0/G1, S and G2/M phases. For cell apoptosis analysis, the cultured cells were stained using annexin V-fluorescein isothiocyanate and propidium iodide (BD Biosciences, USA).

Immunofluorescence assays

Tissues were fixed using 4% paraformaldehyde and embedded in paraffin. The samples were then incubated with primary antibody with PTBP1 at 4 °C overnight and then incubated with goat anti-rabbit IgG with a red or green fluorescent label (Invitrogen, Carlsbad, CA).

Western blot

Protein was extracted from transfected cells with RIPA lysis buffer. Equal amounts of protein samples were loaded and separated by SDS-PAGE and transferred onto PVDF membranes (Merck Millipore, Germany). The membranes were blocked with 5% skim milk in TBST for 1 hour at room temperature. Then, membranes were incubated with diluted primary antibodies anti-PTBP1 for western blot (1:1000 dilutions, 12582-1-AP, Proteintech Group, USA), anti-FASN for western blot (1:1000 dilutions, 10624-2-AP, Proteintech Group, USA) at 4℃ overnight. Then, membranes were washed with TBST three times, 15 minutes/time, followed by incubating with secondary antibody for an hour, washed again with TBST. Finally, the protein bands were visualized by using Gel Doc 2000 (Bio-Rad) and the grey values were measured by Image J software.

Transcription in vitro and RNA pull-down assay

For transcription in vitro, plasmid containing double T7 promoters was digested by single restriction endonuclease. T7 High Yield RNA Transcription Kit (Vazyme, Nanjing, China) was used to transcript forward and reverse linear DNA template to RNA (sense and antisense probe), which was subsequently purified by RNeasy Mini Kit (Qiagen, Germany). Then, Pierce™ RNA 3' End Desthiobiotinylation Kit (Thermo Fisher Scientific, Rockford, USA) was used to label biotin to the 3' End of RNA. For RNA pull-down assay, 1×10^7 cells were washed in ice-cold PBS, lysed in 500 μl co-IP buffer (Thermo Scientific) supplemented with a cocktail of proteinase inhibitors, phosphatase inhibitors, and RNase inhibitor (Invitrogen), then incubated with 3 μg biotinylated DNA oligo probes against sense or antisense for 2 h at room temperature. A total of 50 μl washed Streptavidin magnetic beads (Thermo Fisher Scientific, Rockford, USA) were added to each binding reaction and further incubated for another hour at room temperature. The beads were washed briefly with elution buffer for five times. Finally, the retrieved proteins were used for mass spectrometry or western blot analysis.

Silver staining and mass spectrometry analysis

Silver staining was performed using the Fast Silver Stain Kit (Beyotime, Shanghai, China) as the protocol described, while MS was done by BGI Genomics (Shenzhen, China). The protein identification uses experimental MS/MS data and aligns them with theoretical MS/MS data from database to obtain results. The whole process starts from converting raw MS data into a peak list and then searching matches in the database. The search results are subject to strict filtering and quality control, and possible protein identifications are produced. Finally, from the final protein identification list, functional annotation analysis such as GO, COG/KOG, and Pathway analysis are performed.

RNA immunoprecipitation

RIP experiments were performed with a RNA Immunoprecipitation Kit (Geneseed, Guangzhou, China) according to the manufacturer's instructions. Co-precipitated RNA was detected by qRT-PCR.

Lipidomics

Lipid extraction and mass spectrometry-based lipid detection of cell pellet were followed by experimental operation of Huang et al[25]. A quality control sample was prepared by mixing equal parts of all samples. During the whole experiments, we processed with the same parameters as the analytical sample to evaluate the stability of analytical performance and reliability of data. Ultra-high-performance liquid chromatograph-mass spectrometry analysis was performed on Q Exactive Plus high-resolution mass spectrometer (Thermo Scientific, USA) equipped with an Ultimate 3000 UHPLC system (Thermo Scientific, USA). Lipid identification (structural identification) and a peak table containing the retention time, m/z, peak area (peak matching) were assessed with the MS-DIAL software. The data combination of positive and negative ion modes was defined as relative lipid abundance for subsequent statistical analysis.

Co-Immunoprecipitation

To detect protein–protein interactions, cells were lysed in 500 μl co-IP buffer supplemented with a cocktail of proteinase inhibitors, phosphatase inhibitors, and RNase inhibitor. The lysates were centrifuged at 12,000g for 30 min, and the supernatant was used for immunoprecipitation with agarose beads, which were preincubated with the corresponding antibodies. After incubation at 4 °C overnight, beads were washed three times with PBS. SDS sample buffer was added to the agarose beads and the immunoprecipitates were used for western blot analysis.

Statistical analysis

Results were shown as the mean ± SD. SPSS 22.0 (IBM Corp., Armonk, NY, USA), R 4.0.5 and GraphPad Prism 8.0 were used for comparison analysis. Student t-test was used for comparison between two groups. The Chi-squared test was used for the association of the expression of circMBOAT2 with patients' clinic pathological parameters. $P < 0.05$ were considered statistically significant.

Results

CircMBOAT2 is an upregulated circRNA associated with lipid metabolism in ICC

Metabolism reprogramming is a hallmark of cancer, no except for ICC[26]. We analyzed expression profiles of circRNAs in five paired samples of ICC by RNA-seq. A total of 95 dysregulated circRNAs meeting the following requirements: (1) the |average normalized fold change| ≥2; (2) P value <0.05 were identified in ICC tissues (Additional file 3. Supplementary Table 1), of which 26 circRNAs were upregulated and 69 circRNAs were downregulated (Fig. 1A and B). Next, gene functions of the selected circRNAs associated with lipid metabolism were identified by Gene ontology (GO) term and Kyoto Encyclopedia of Genes and Genomes (KEGG) pathway assignments. Interestingly, only circMBOAT2 (has_circ_0007334 in circBase) expression is related to lipid biosynthesis and metabolism. Then we conform the differential expression between ICC and normal biliary tissues/cells (Fig. 1C and D). We next analyzed correlation between circMBOAT2 expression and clinicopathologic features in patients with ICC and found that high expression of circMBOAT2 was positively associated with tumor size in ICC patients (Additional file 4. Supplementary Table 2).

circMBOAT2 is generated from the exons 2–3 of MBOAT2 gene with a length of 224nt. The backsplice junction site and full length of circMBOAT2 was amplified using divergent and convergent primers then confirmed by Sanger sequencing (Fig. 1E). The sequence is keeping with circBase database annotation (http://www.circbase.org/). PCR analysis showed that circMBOAT2 could be amplified by divergent primers in gDNA, cDNA reverse transcribed from random hexamers, and oligo(dT) primers. However, circMBOAT2 could only be amplified by convergent primers in cDNA reverse transcribed from random hexamers instead of gDNA or cDNA reverse transcribed from oligo(dT) primers (Fig. 1F). Resistance to digestion with RNase R exonuclease demonstrated that circMBOAT2 harbors a closed loop structure (Fig. 1G). Nuclear and cytoplasmic fractionation and fluorescence in situ hybridization (FISH) examination revealed that circMBOAT2 was localized both in the cytoplasm and in the nucleus (Fig. 1H and I).

Therefore, these results demonstrate that circMBOAT2 is a bona fide circRNA abundantly distributed in ICC.

CircMBOAT2 promotes ICC progression

To study the functional role of circMBOAT2 in ICC progression, we measured the endogenous expression of circMBOAT2 in seven cell lines. Results showed that the expression of circMBOAT2 is higher in QBC-939, HCCC-9810, RBE, CCLP1 as well as FRH cells than H69 cells, a sort of normal biliary epithelial cell (Fig. 1D). We used RBE and HCCC-9810 cells in following experiment because they are universally acknowledged and reserved in ATCC cell repository. Furthermore, we used double sets of small-interfering RNAs (siRNAs) si-circMBOAT2#1 and si-circMBOAT2#2 specifically targeting the junction site of circMBOAT2, which significantly reduced the expression of circMBOAT2 in RBE cells (Supplementary Fig. S1A). Therefore, si-circMBOAT2#1 and si-circMBOAT2#2 were used for the following loss-of-function assays of circMBOAT2. For circNDUFB2 overexpression, we constructed circMBOAT2 overexpression plasmid (Supplementary Fig. S1B), and confirmed circMBOAT2 was overexpressed accurately and efficiently in ICC cells (Supplementary Fig. S1C). These results indicate that MBOAT2 is unaffected by circMBOAT2.

Biological functions of knockdown and overexpression lines were further measured using the Cell Counting Kit-8 (CCK-8), colony formation, EdU cell proliferation assay, as well as flow cytometry. These revealed that circMBOAT2 knockdown inhibits cell proliferation, colony formation, but promotes both the early and late stages of apoptosis and G0/G1 cell cycle arrest in RBE and HCCC-9810 cells (Fig. 2A-E). Whereas, these activities are contrary to circMBOAT2 knockdown when circMBOAT2 is overexpressed in RBE cells (Supplementary Fig. S2A-S2D). Taken together, these findings indicated that circMBOAT2 could promote ICC growth.

CircMBOAT2 regulates lipid metabolism reprogramming especially unsaturated lipid

Cause circMBOAT2 expression is related to lipid biosynthesis and metabolism from the analysis results shown in RNA-seq, we used the BODIPY493/503 probe to detect the neutral lipid droplet content in ICC cells. The results indicate that the content of neutral lipid droplet was reduced after circMBOAT2 knockdown (Fig. 3A and B). Then, we performed RNA-seq and untargeted lipid metabolomics (lipidomics) analysis on circMBOAT2-knockdown cells, to validate our findings that circMBOAT2 modulates lipid metabolism reprogramming in ICC. Gene set enrichment analysis (GSEA) showed that the biosynthesis of unsaturated fatty acids pathway-related genes were affected in HCCC-9810 cells with circMBOAT2 KD (Fig. 3C). Untargeted lipidomics identified 474 lipids belonging to 14 lipid classes (Additional file 5. Supplementary Table 3, Fig. 3D). Principal component analysis (PCA) results showed that the lipidomics of HCCC-9810 cells with circMBOAT2 KD was quite different compared with negative control transfected cells (Fig. 3E). The changed lipid species in circMBOAT2 knockdown HCCC-9810 cells were shown (Fig. 3F), unsaturated lipid has an obvious change than saturated lipid. Therefore, our data suggest that circMBOAT2 promotes ICC lipid metabolism reprogramming, especially unsaturated lipid metabolism reprogramming, which could be a characteristic in ICC progression.

CircMBOAT2 interacts with PTBP1 in ICC cells

To test if circMBOAT2 regulates downstream as an miRNA sponge in ICC, we conducted RIP assay. Result showed that circMBOAT2 was not significantly enriched by the AGO2 antibody (Fig. S3A and S3B), suggests that circMBOAT2 may not affect as an miRNA sponge in ICC progression. Then, we examined if circMBOAT2 could be translated to protein via an online database (http://lilab.research.bcm.edu/). Result showed that circMBOAT2 has extremely low potential to code (Fig. S3C). To explore whether circMBOAT2 fulfilled function by interacting with proteins, we conducted RNA pull-down assay to explore the proteins associated with it. The precipitated proteins in RNA pull-down assay were separated by 10% SDS-PAGE then detected by silver staining (Fig. 4A). LC-MS/MS was used to identify the proteins pulled down by the circMBOAT2 probe, and the results are presented in Additional file 6. Supplementary Table 4 and Fig. 4B. Among the proteins, fatty acid synthetase (FASN) was found to be a lipid metabolism associated protein, whereas it binds to both sense and antisense probe. Another RNA binding protein polypyrimidine tract binding protein 1 (PTBP1), reported that could regulate metabolism reprogramming[27], interacts with sense probe specifically. Of note, AGO2 was not found in the precipitates, which further confirmed that circMBOAT2 does not function through ceRNA mechanism. We following performed western blot analysis, which is consistent to the outcome of LC-MS/MS (Fig. 4C). Using RIP assay, we confirmed that PTBP1 binds to circMBOAT2 specifically instead of FASN (Fig. 4D and 4E, Fig. S3D and S3E). In addition, we performed RNA FISH immunofluorescence assay and found circMBOAT2 colocalized with PTBP1 in both of the cytoplasm and nucleus (Fig. 4F). Taken together, these results indicate that circMBOAT2 performs a function via binding to PTBP1.

CircMBOAT2 protects PTBP1 from ubiquitin/proteasome-dependent degradation

Western blot analyses in RBE and HCCC-9810 cells was performed to further examine the relationship between circMBOAT2 and PTBP1. Results showed that circMBOAT2 knockdown reduces PTBP1 protein level, and on the contrary, circMBOAT2 overexpression increases PTBP1 protein level (Fig. 5A-B). Notably, FASN protein level was increased under circMBOAT2 overexpression, indicates that FASN may be regulated in an indirect manner (Fig. 5B). Therefore, we speculated that circMBOAT2 may stabilize PTBP1 protein through interaction. Ubiquitin/proteasome-dependent degradation is the most common degradation pathway in eukaryocyte[28]. Hence, we investigate that circMBOAT2 knockdown significantly reduced the levels of PTBP1 protein, which could be restored by MG132, a specific proteasome inhibitor (Fig. 5C). Furthermore, immunoprecipitation assay was performed and we found that circMBOAT2 knockdown significantly increased the ubiquitination levels of PTBP1 (Fig. 5D and E). These results demonstrate that circMBOAT2 increases the stability of PTBP1 via protecting it from ubiquitin/proteasome-dependent degradation.

CircMBOAT2 promotes PTBP1-mediated cytoplasmic export of FASN mRNA

As a sort of RBP, previous studies have shown that PTBP1 could mediate RNA splicing, and act as a regulator of glycolysis and tumorigenesis[29]. Above results showed that FASN protein level was increased

under circMBOAT2 overexpression (Fig. 5B), as a consequence of which, we inspected that PTBP1 could bind with FASN mRNA. By performing RIP assay, we confirmed that PTBP1 can bind with FASN mRNA (Fig. 6A). In order to investigate the function of PTBP1 after binding with FASN mRNA, we detected the level of FASN mRNA in condition of PTBP1 knockdown via two sets of siRNAs (si-PTBP1#1 and si-PTBP1#2) and found that there was no significant difference after PTBP1 knockdown (Fig. 6B). However, protein level of FASN was reduced after PTBP1 knockdown in RBE and HCCC-9810 cells (Fig. 6C). Coincident with the performance in ICC cell lines, comparing with adjacent non-tumor tissues, the RNA level of FASN has no significant difference between ICC tissues and normal tissues adjacent to ICC tissues (Fig. 6D). These results demonstrated that PTBP1 doesn't mediate FASN mRNA splicing. Then, we speculated that PTBP1 could promote the cytoplasmic export of FASN mRNA. To prove the hypothesis, nuclear and cytoplasmic fractionation and fluorescence in situ hybridization (FISH) examination was performed. Interestingly, we observed a clear reduction of cytoplasmic FASN mRNA levels in RBE and HCCC-9810 cells upon PTBP1 knockdown (Fig. 6E-F). We further detected the effects of PTBP1 knockdown on FASN expression. PTBP1 knockdown abrogated the effect of overexpressed circMBOAT2 on FASN expression in RBE cells (Fig. 6G). These results revealed that circMBOAT2 promoted FASN mRNA cytoplasmic export and expression by interacting with PTBP1 in ICC cells.

CircMBOAT2 promotes lipid metabolism reprogramming and progression in ICC through FASN

We then investigated if the role of circMBOAT2 in progression of ICC is dependent on the FASN pathway. The efficiency of three sets of siRNAs si-FASN#1, si-FASN#2 and si-FASN#3 was tested, all of them could reduce the expression of FASN (Fig. 7A). Si-FASN#2 and si-FASN#3, which were more efficient, were used in following assays. In vitro assays by the Cell Counting Kit-8 (CCK-8), EdU cell proliferation assays, as well as flow cytometry demonstrated that reduced expression of FASN functionally inhibits cell proliferation and promotes both the early and late stages of apoptosis and G0/G1 cell cycle arrest in RBE and HCCC-9810 cells (Fig. 7B-E). To further prove the role of FASN in progression of ICC, an FASN suppressive pharmaceutical TVB-2640(Denifanstat) was used. Consistent with the results in functional assays by siRNA, TVB-2640 could inhibit cell proliferation and promotes both the early and late stages of apoptosis and G0/G1 cell cycle arrest in HCCC-9810 cells (Fig. S4A-S4C).

We next compared the lipid levels among control, circMBOAT2-silenced or FASN-silenced ICC cells by lipidomics. PCA analysis indicated that downregulation of FASN in ICC cells was parallel with that of circMBOAT2 silencing (Fig. 7F). The changed lipid species in circMBOAT2-silenced and FASN-silenced ICC cells were shown (Fig. S5A). In terms of fatty acids, semblable changes occurred in circMBOAT2-silenced or FASN-silenced ICC cells (Fig. S5B). Except for C16:0, no significant differences of saturated fatty acids were found, while unsaturated fatty acids were different and the trend is more obvious in unsaturated fatty acids with more unsaturated bonds or with fewer carbons (Fig. S5C and S5D). These data suggest that the lipid metabolism reprogramming functions of circMBOAT2 in promoting ICC cell progression rely on the FASN pathway. All together, these results demonstrated that FASN could promote ICC progression and lipid metabolism reprogramming, which was regulated by the circMBOAT2/PTBP1 axis (Fig. 7G).

Arachidonic acid (C20:4) and adrenic acid (C22:4) intervene ICC progression in circMBOAT2/PTBP1/FASN axis

PUFAs are essential for the formation of cell membrane phospholipids, which are required for the rapid proliferation of cancer cells[30]. It was reported that n-6 polyunsaturated fatty acids (PUFAs) intake is associated with an elevated proportion of eicosanoids with carcinogenic effects[31]. Based on our lipidomics results above (Additional file 5. Supplementary Table 3), we found that the proportion of two sorts of n-6 PUFAs, arachidonic acid (C20:4) and adrenic acid (C22:4), were significantly reduced in the circMBOAT2-silenced and FASN-silenced group (Fig. 5D), as a consequence of which, we explored the function of these two n-6 PUFAs in FASN-mediated ICC progression. In vitro, Cell Counting Kit-8 (CCK-8), EdU cell proliferation assays, as well as flow cytometry demonstrated that reduced expression of FASN functionally inhibits cell proliferation and promotes both the early and late stages of apoptosis and G0/G1 cell cycle arrest in HCCC-9810 cells, which could be reversed by additional arachidonic acid and adrenic acid supplements (Fig. S6A-S6C). This tentatively indicated a possible role for arachidonic acid and adrenic acid in the carcinogenicity of FASN in ICC.

Discussion

CircRNAs have been discovered more than 45 years, however, they were considered as accessory substances generated by abnormal splicing with little functional potential until 2013[32,33]. Increasing evidence suggests that circRNAs are dysregulated in multiple cancers, and their atypical function in regulating cancer cell proliferation, migration, invasion and metastasis renders them potential biomarkers and therapeutic targets[32]. Aberrant regulation of circRNAs were also proposed to be involved in clinical cancer treatment resistance, which includes standard chemotherapy, targeted therapy and immunotherapy[34]. Nonetheless, the molecular mechanism of circRNAs in ICC remains largely unclear. An earlier study showed that hsa_circ_0021205 could suppress ICC progression by sponging miR-204-5p[35]. Even more interestingly, circGGNBP2 is able to encode a small non-featured peptide, cGGNBP2-184aa, and it is cGGNBP2-184aa rather than circGGNBP2 that promotes cell growth and metastasis in ICC[5]. In the present study, we performed whole transcriptome sequencing and found that circMBOAT2 was frequently downregulated in ICC tissues. CircMBOAT2 not only directly bound to PTBP1 to prevent it from ubiquitinated degradation, but also eliciting ICC lipid metabolism reprogramming by facilitating FASN translation. We report for the first time that circMBOAT2 promotes ICC progression by stabilizing PTBP1 and activating the lipid metabolism reprogramming.

Increasing evidence suggests that the expression levels of circRNA are related to the clinicopathological characteristics of tumor patients[34]. We found that circMBOAT2 decrease was significantly associated with tumor size in ICC patients (Supplementary Data 2). At the time of our study, however, we noted that the majority of patients (23/26) were hepatitis-free. The prevalence of hepatitis in our cohort differs from the typical circumstances of ICC that 27% of ICC patients in the U.S. have hepatitis virus infection and 22.5% with HBV infection in China[1,36]. Hence, whether circMBOAT2 expression is associated with

hepatitis virus infection in ICC patients needs to be further investigated by expanding the sample size of the cohort. In addition, oncogenic driver mutations or gene rearrangements in ICC are gradually gained attention. IDH1/2 and FGFR mutations have been reported to occur at frequencies of 10–20% and 10–15% in ICC, and the corresponding targeted therapeutics, Ivosidenib and Pemigatinib, have been preliminarily shown to be effective in clinical trials[37,38]. However, the correlation of IDH1/2 and FGFR mutation status with circMBOAT2 is unclear and needs further investigation.

ICC is the second most common primary liver tumor with limited therapeutic options. Despite advances in the comprehensive therapeutic of patients, the prognosis has not improved significantly over the past decades, with a 5-year survival rate of approximately 22–44% after resection[4]. New strategies are therefore urgently needed to improve the prognosis of patients with ICC. Deregulating cellular metabolism were segregated as “emerging hallmarks” in the Hallmarks of Cancer[17], which could be a new strategy for curing ICC. In our study, we successfully identified the metabolism-related circRNA circMBOAT2 from RNA-seq data of ICC tissues, which is one of the overexpressed circRNAs and has also been shown to correlate with tumor size in clinical specimens. In the following functional assays, circMBOAT2 significantly facilitated proliferation, colony formation in ICC cells, but prevented them from both the early and late stages of apoptosis and G0/G1 cell cycle arrest. Based on the findings above, the oncogenic role of circMBOAT2 in ICC, especially the proliferative phenotype, was robustly confirmed.

Previously, all studies focused on the role of circMBOAT2 as a miRNA sponge[39,40]. In the present study, by performing RNA pull-down assay and LC-MS/MS analysis, we demonstrated that circMBOAT2 does not exert its function through a ceRNA mechanism, but enhances the stability of PTBP1, a sort of ribosomal protein by binding to it. We subsequently investigated the relationship between circMBOAT2 and PTBP1 and found that cirMBOAT2 protects PTBP1 from degradation by reducing ubiquitin-mediated proteolysis for the first time, thereby enhancing its activity. However, it is unclear whether circMBOAT2 directly inhibits ubiquitination of PTBP1 by competitively binding to a ubiquitin ligase recognition domain, or acts as a scaffold that provides a platform for the interaction between PTBP1 and specific deubiquitination-associated proteins. Therefore, this key question requires further investigate.

As a sort of ribosomal protein, PTBP1 promotes the development of various types of cancer by intensifying the stability of mRNA or translation of oncogenic factors[29]. However, there is little knowledge about the function of PTBP1 in regulating the cytoplasmic export of RNA in cancer cells. Meanwhile, the role of PTBP1 in ICC has not been investigated before. In the present study, by RIP experiments, we found that PTBP1 was able to bind to FASN mRNA and transport it to the cytoplasm and then translate. This discovery enriches the literature that PTBP1 regulates RNA subcellular localization and fulfills a gap in the study of PTBP1 in ICC.

It is widely perceived that fatty acids (FAs) are critical for cancer cells as they maintain membrane biosynthesis during rapid cell proliferation and supply an important source of energy under conditions of metabolic stress. In Addition, FAs and their by-products have been found to act as secondary messengers for signal transduction or to directly regulate intracellular homeostasis by modulating the surrounding

microenvironment to create conditions favorable for tumor progression[41]. Thereby, suppression of FAs metabolic pathways is a reasonable option for tumor therapeutic. Notably, FASN plays an essential role in the de novo synthesis of FAs, of which palmitate (C16:0) is the major product, and can generate additional FAs species through the prolongation and desaturation of SCDs, ELOVLs and FADs. The conversion of the lipid synthesis transcriptional regulator SREBP1 to its mature active form is strongly impacted by a PI3K-AKT-mTORC1-dependent mechanism; thus, the expression of pivotal lipogenic enzymes, such as FASN, is inhibited when mTORC1 is blocked by rapamycin or Raptor knockdown[42]. Nevertheless, the mechanism of post-transcriptional regulation of FASN is unknown. In the present investigation, we inhibited FASN by down-regulating circMBOAT2 levels and observed similar effects to direct knockdown of FASN in ICC proliferation and lipid metabolism. Hence, our findings support the hypothesis that circMBOAT2 is a promising target for cancer therapy. Remarkably, we found that FASN-block effectively inhibited ICC progression in vitro, suggesting that it may have beneficial effects in patients with circMBOAT2-associated ICC (i.e., patients with elevated levels of circMBOAT2 expression). Importantly, however, although FASN-block-mediated inhibition of metabolic activity is consistent with that in circMBOAT2 knockdown ICC cells, its specific mechanism may be complicated and requires further study.

In our study, we also found that the FASN-block mostly affected the levels of unsaturated fatty acids (UFAs), especially polyunsaturated fatty acids (PUFAs) in ICC cells, while the levels of saturated fatty acids (SFAs) were less affected by it. PUFAs were previously reported to be preferentially incorporated and predominantly metabolized in colorectal cancer cells, with more PUFAs compared to normal intestinal mucosa[43], which is consistent with our findings. One of the probable reasons is that PUFAs are essential for the formation of cell membrane phospholipids during the rapid proliferation of cancer cells. On the flip side, results from in vitro and in vivo studies concluded that PUFAs may have anti-cancer properties. The consuming of n-3 UFAs reduced the risk of various cancers, including breast[44], colon[45], prostate[46], leukemia[47] and melanoma[48]. The addition of n-3 PUFAs to the diet inhibited inflammatory processes, stimulated apoptosis, suppressed metastasis and tumor proliferation, and upregulated gene expression of antioxidant enzymes. In contrast, the intake of n-6 PUFAs was associated with an increased proportion of eicosanoids, which were carcinogenic[30]. The explanation may be that n-3 and n-6 PUFAs have contrasting effects on the progression of cancer, however, their roles in ICC progression remain to be further investigated.

Conclusions

In conclusively, our study suggests for the first time that lipid metabolic reprogramming in ICC is regulated by circMBOAT2, which is associated with its progression. Mechanistically, we first found that circMBOAT2 bound to and stabilized PTBP1, thereby contributing to the cytoplasmic export of FASN mRNA. Importantly, our findings suggested that silencing circMBOAT2 offers a new therapeutic strategy for the treatment of ICC, especially that with active lipid metabolism.

Abbreviations

ICC
Intrahepatic cholangiocarcinoma
FASN
fatty acid synthetase
CircRNAs
Circular RNAs
RNA-seq
RNA sequencing
cDNA
Complementary DNA
gDNA
Genomic DNA
qRT-PCR
Quantitative real-time PCR
SDS/PAGE
SDS polyacrylamide gel electrophoresis
FISH
Fluorescent in situ hybridization
siRNA
Short interfering RNA
PTBP1
Polypyrimidine Tract Binding Protein 1.

Declarations

Acknowledgements

Not applicable

Authors' contributions

Zhaohui Tang and Shouhua Wang conceived the project and supervised the project. Xiaopeng Yu, Huanjun Tong, Jialu Chen and Shuqing Wang performed the biological experiments. Chenwei Tang and Yu Si collected the clinical data. Xiaopeng Yu analyzed data and wrote the manuscript. All the authors read and approved the final manuscript.

Funding

This research was supported by the National Natural Science Foundation of China (Grant Number 81772521) and sponsored by Multicenter Clinical Research Project of Shanghai Jiaotong University

School of Medicine (DLY201807).

Availability of data and materials

The datasets used and/or analyzed during the current study are available from the corresponding author upon reasonable request.

Ethics approval and consent to participate

The present study was approved by the ethics committee of Xinhua Hospital. Written informed consent was obtained from all patients and conducted in accordance with the Declaration of Helsinki.

Consent for publication

Not applicable.

Competing interests

The authors declare that they have no competing interests.

Author details

[1] Department of General Surgery, Xinhua Hospital, Shanghai Jiao Tong University School of Medicine, Shanghai 200092, China. [2] Shanghai Key Laboratory of Biliary Tract Disease Research, Xinhua Hospital, Shanghai Jiao Tong University School of Medicine, Shanghai 200092, China. [3] Department of Blood Transfusion, Xinhua Hospital, Shanghai Jiao Tong University School of Medicine, Shanghai 200092, China.

References

1. Gupta A, Dixon E. Epidemiology and risk factors: intrahepatic cholangiocarcinoma. *Hepatobiliary Surg Nutr.* 2017;6(2):101-104.
2. Yamasaki S. Intrahepatic cholangiocarcinoma: macroscopic type and stage classification. *J Hepatobiliary Pancreat Surg.* 2003;10(4):288-291.
3. Bragazzi MC, Ridola L, Safarikia S, et al. New insights into cholangiocarcinoma: multiple stems and related cell lineages of origin. *Ann Gastroenterol.* 2018;31(1):42-55.
4. Banales JM, Cardinale V, Carpino G, et al. Expert consensus document: Cholangiocarcinoma: current knowledge and future perspectives consensus statement from the European Network for the Study of Cholangiocarcinoma (ENS-CCA). *Nat Rev Gastroenterol Hepatol.* 2016;13(5):261-280.
5. Li H, Lan T, Liu H, et al. IL-6-induced cGGNBP2 encodes a protein to promote cell growth and metastasis in intrahepatic cholangiocarcinoma. *Hepatology.* 2021.

6. Chen Q, Wang H, Li Z, et al. Circular RNA ACTN4 promotes intrahepatic cholangiocarcinoma progression by recruiting YBX1 to initiate FZD7 transcription. *J Hepatol.* 2022;76(1):135-147.
7. Ashwal-Fluss R, Meyer M, Pamudurti NR, et al. circRNA biogenesis competes with pre-mRNA splicing. *Mol Cell.* 2014;56(1):55-66.
8. Li J, Gao X, Zhang Z, et al. CircCD44 plays oncogenic roles in triple-negative breast cancer by modulating the miR-502-5p/KRAS and IGF2BP2/Myc axes. *Mol Cancer.* 2021;20(1):138.
9. Yu J, Xu QG, Wang ZG, et al. Circular RNA cSMARCA5 inhibits growth and metastasis in hepatocellular carcinoma. *J Hepatol.* 2018;68(6):1214-1227.
10. Li B, Zhu L, Lu C, et al. circNDUFB2 inhibits non-small cell lung cancer progression via destabilizing IGF2BPs and activating anti-tumor immunity. *Nature communications.* 2021;12(1):295.
11. Gong W, Xu J, Wang Y, et al. Nuclear genome-derived circular RNA circPUM1 localizes in mitochondria and regulates oxidative phosphorylation in esophageal squamous cell carcinoma. *Signal Transduct Target Ther.* 2022;7(1):40.
12. Cocquerelle C, Mascrez B, Hétuin D, Bailleul B. Mis-splicing yields circular RNA molecules. *Faseb j.* 1993;7(1):155-160.
13. Guo XY, Liu TT, Zhu WJ, et al. CircKDM4B suppresses breast cancer progression via the miR-675/NEDD4L axis. *Oncogene.* 2022.
14. Jia L, Wang Y, Wang CY. circFAT1 Promotes Cancer Stemness and Immune Evasion by Promoting STAT3 Activation. *Adv Sci (Weinh).* 2021;8(13):2003376.
15. Gao X, Xia X, Li F, et al. Circular RNA-encoded oncogenic E-cadherin variant promotes glioblastoma tumorigenicity through activation of EGFR-STAT3 signalling. *Nat Cell Biol.* 2021;23(3):278-291.
16. Faubert B, Solmonson A, DeBerardinis RJ. Metabolic reprogramming and cancer progression. *Science.* 2020;368(6487).
17. Hanahan D. Hallmarks of Cancer: New Dimensions. *Cancer Discov.* 2022;12(1):31-46.
18. Zou S, Li J, Zhou H, et al. Mutational landscape of intrahepatic cholangiocarcinoma. *Nat Commun.* 2014;5:5696.
19. Thamrongwaranggoon U, Seubwai W, Phoomak C, et al. Targeting hexokinase II as a possible therapy for cholangiocarcinoma. *Biochem Biophys Res Commun.* 2017;484(2):409-415.
20. Breast Cancer Brain Metastases Rely on FASN-Mediated Lipid Biosynthesis. *Cancer Discov.* 2021;11(6):1315.
21. Jiang L, Fang X, Wang H, Li D, Wang X. Ovarian Cancer-Intrinsic Fatty Acid Synthase Prevents Anti-tumor Immunity by Disrupting Tumor-Infiltrating Dendritic Cells. *Front Immunol.* 2018;9:2927.
22. Gu L, Zhu Y, Lin X, Tan X, Lu B, Li Y. Stabilization of FASN by ACAT1-mediated GNPAT acetylation promotes lipid metabolism and hepatocarcinogenesis. *Oncogene.* 2020;39(11):2437-2449.
23. Jin Y, Chen Z, Dong J, et al. SREBP1/FASN/cholesterol axis facilitates radioresistance in colorectal cancer. *FEBS Open Bio.* 2021.

24. Tomacha J, Dokduang H, Padthaisong S, et al. Targeting Fatty Acid Synthase Modulates Metabolic Pathways and Inhibits Cholangiocarcinoma Cell Progression. *Front Pharmacol.* 2021;12:696961.
25. Huang H, Ye G, Lai SQ, et al. Plasma Lipidomics Identifies Unique Lipid Signatures and Potential Biomarkers for Patients With Aortic Dissection. *Front Cardiovasc Med.* 2021;8:757022.
26. Satriano L, Lewinska M, Rodrigues PM, Banales JM, Andersen JB. Metabolic rearrangements in primary liver cancers: cause and consequences. *Nat Rev Gastroenterol Hepatol.* 2019;16(12):748-766.
27. Yang Y, Ren P, Liu X, et al. PPP1R26 drives hepatocellular carcinoma progression by controlling glycolysis and epithelial-mesenchymal transition. *J Exp Clin Cancer Res.* 2022;41(1):101.
28. Wang J, Maldonado MA. The ubiquitin-proteasome system and its role in inflammatory and autoimmune diseases. *Cell Mol Immunol.* 2006;3(4):255-261.
29. Zhu W, Zhou BL, Rong LJ, et al. Roles of PTBP1 in alternative splicing, glycolysis, and oncogensis. *J Zhejiang Univ Sci B.* 2020;21(2):122-136.
30. Liput KP, Lepczyński A, Ogłuszka M, et al. Effects of Dietary n-3 and n-6 Polyunsaturated Fatty Acids in Inflammation and Cancerogenesis. *Int J Mol Sci.* 2021;22(13).
31. Zanoaga O, Jurj A, Raduly L, et al. Implications of dietary ω-3 and ω-6 polyunsaturated fatty acids in breast cancer. *Exp Ther Med.* 2018;15(2):1167-1176.
32. Kristensen LS, Andersen MS, Stagsted LVW, Ebbesen KK, Hansen TB, Kjems J. The biogenesis, biology and characterization of circular RNAs. *Nat Rev Genet.* 2019;20(11):675-691.
33. Memczak S, Jens M, Elefsinioti A, et al. Circular RNAs are a large class of animal RNAs with regulatory potency. *Nature.* 2013;495(7441):333-338.
34. Lu JC, Zhang PF, Huang XY, et al. Amplification of spatially isolated adenosine pathway by tumor-macrophage interaction induces anti-PD1 resistance in hepatocellular carcinoma. *J Hematol Oncol.* 2021;14(1):200.
35. Tu J, Chen W, Zheng L, et al. Circular RNA Circ0021205 Promotes Cholangiocarcinoma Progression Through MiR-204-5p/RAB22A Axis. *Front Cell Dev Biol.* 2021;9:653207.
36. Wu Q, He XD, Yu L, Liu W, Tao LY. The metabolic syndrome and risk factors for biliary tract cancer: a case-control study in China. *Asian Pac J Cancer Prev.* 2012;13(5):1963-1969.
37. Casak SJ, Pradhan S, Fashoyin-Aje LA, et al. FDA Approval Summary: Ivosidenib for the treatment of patients with advanced unresectable or metastatic, chemotherapy refractory cholangiocarcinoma with an IDH1 mutation. *Clin Cancer Res.* 2022.
38. Abou-Alfa GK, Sahai V, Hollebecque A, et al. Pemigatinib for previously treated, locally advanced or metastatic cholangiocarcinoma: a multicentre, open-label, phase 2 study. *Lancet Oncol.* 2020;21(5):671-684.
39. Yu K, Liu M, Huang Y, et al. circMBOAT2 serves as the sponge of miR-433-3p to promote the progression of bladder cancer. *Pathol Res Pract.* 2021;227:153613.

40. Zhou X, Liu K, Cui J, et al. Circ-MBOAT2 knockdown represses tumor progression and glutamine catabolism by miR-433-3p/GOT1 axis in pancreatic cancer. *J Exp Clin Cancer Res.* 2021;40(1):124.
41. Koundouros N, Poulogiannis G. Reprogramming of fatty acid metabolism in cancer. *Br J Cancer.* 2020;122(1):4-22.
42. Ricoult SJ, Yecies JL, Ben-Sahra I, Manning BD. Oncogenic PI3K and K-Ras stimulate de novo lipid synthesis through mTORC1 and SREBP. *Oncogene.* 2016;35(10):1250-1260.
43. Mika A, Kobiela J, Pakiet A, et al. Preferential uptake of polyunsaturated fatty acids by colorectal cancer cells. *Sci Rep.* 2020;10(1):1954.
44. Chen J, Stavro PM, Thompson LU. Dietary flaxseed inhibits human breast cancer growth and metastasis and downregulates expression of insulin-like growth factor and epidermal growth factor receptor. *Nutr Cancer.* 2002;43(2):187-192.
45. Chamberland JP, Moon HS. Down-regulation of malignant potential by alpha linolenic acid in human and mouse colon cancer cells. *Fam Cancer.* 2015;14(1):25-30.
46. Lloyd JC, Masko EM, Wu C, et al. Fish oil slows prostate cancer xenograft growth relative to other dietary fats and is associated with decreased mitochondrial and insulin pathway gene expression. *Prostate Cancer Prostatic Dis.* 2013;16(4):285-291.
47. Arita K, Kobuchi H, Utsumi T, et al. Mechanism of apoptosis in HL-60 cells induced by n-3 and n-6 polyunsaturated fatty acids. *Biochem Pharmacol.* 2001;62(7):821-828.
48. Yamada H, Hakozaki M, Uemura A, Yamashita T. Effect of fatty acids on melanogenesis and tumor cell growth in melanoma cells. *J Lipid Res.* 2019;60(9):1491-1502.

Figures

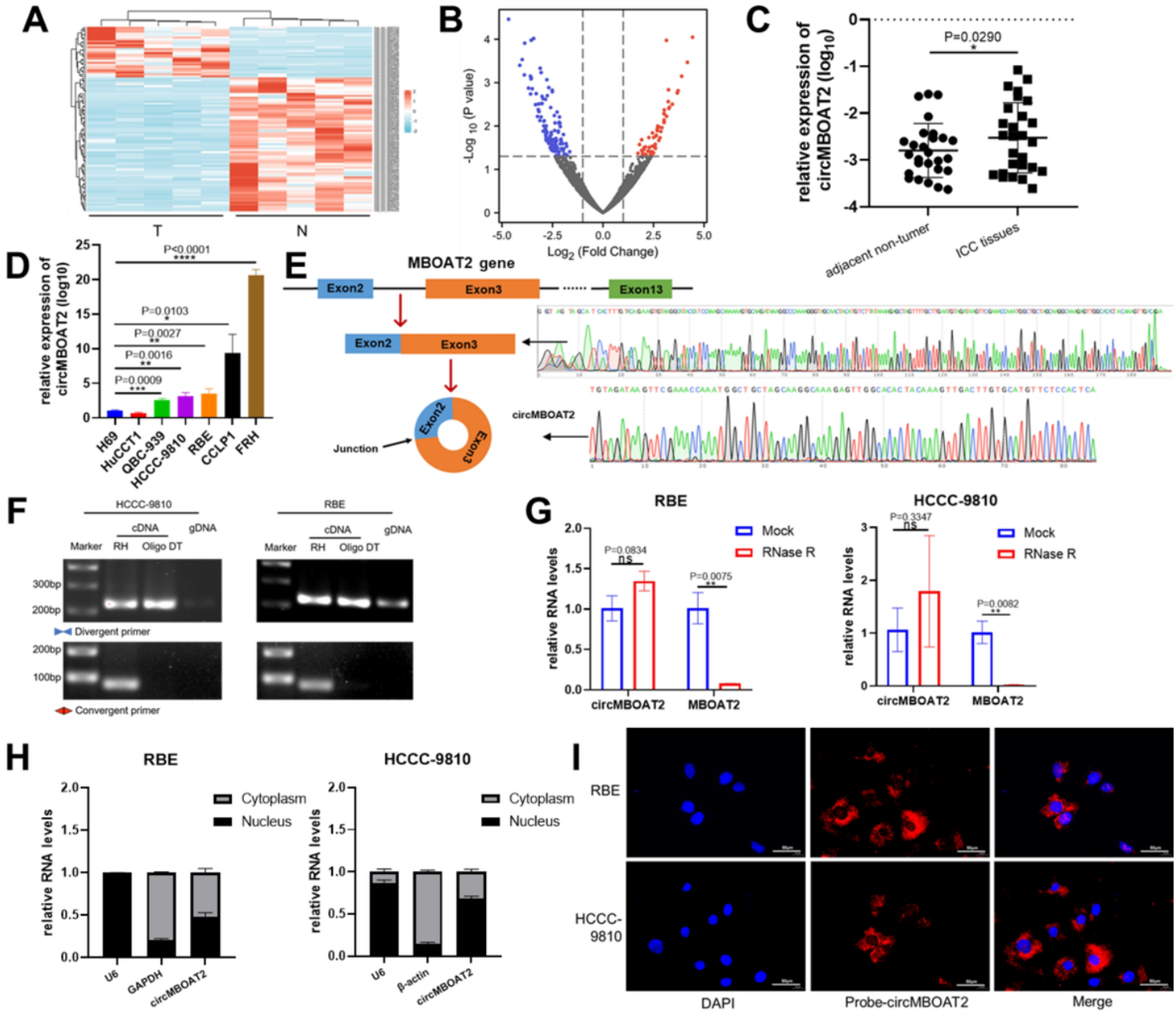

Figure 1

CircMBOAT2 is an upregulated circRNA associated with lipid metabolism in ICC. **a, b** The heat map showed that there were 26 up-regulated and 69 down-regulated circRNAs in ICC tissue compared to adjacent non-tumor tissue by RNA sequencing analysis. **c** The qRT-PCR method was applied to detect the expression levels of circMBOAT2 in 26 ICC patients and normal tissues adjacent to the cancer. The expression of circMBOAT2 was normalized to β-actin. Significant differences between groups were analyzed by paired sample t-test. **d** The relative expression of circMBOAT2 in six human ICC cell lines and one human normal bile duct epithelial cell line (H69) by qRT-PCR. **e** Explanation of the illustrated genomic loci of MBOAT2 and validation strategy for circular exons 2-3 (circMBOAT2). Sanger sequencing after PCR revealed MBOAT2 exons 2-3 and "head and tail" splicing of circMBOAT2. **f** PCR analysis of circMBOAT2 by divergent primers and convergent primers in cDNA and genomic DNA. RH random

hexamers, OdT oligo(dT)18 primers, gDNA genomic DNA. **g** Relative RNA levels of RNase R-treated circMBOAT2 and linear MBOAT2. **h** Relative RNA levels of circMBOAT2 and linear MBOAT2 at different time points of actinomycin D treatment. **i** The nuclear and cytoplasmic fractions were obtained by isolation. circMBOAT2 is mainly localized in the nucleus. U6 is abundantly expressed in the nucleus and GAPDH or β-actin is mainly present in the cytoplasm and served as a nuclear and cytoplasmic RNA marker. **j** Fluorescence in situ hybridization (FISH) of RNA was performed on circMBOAT2. Nuclei were stained with 4,6-diamino-2-phenylindole (DAPI). Scale bar = 50 μm.

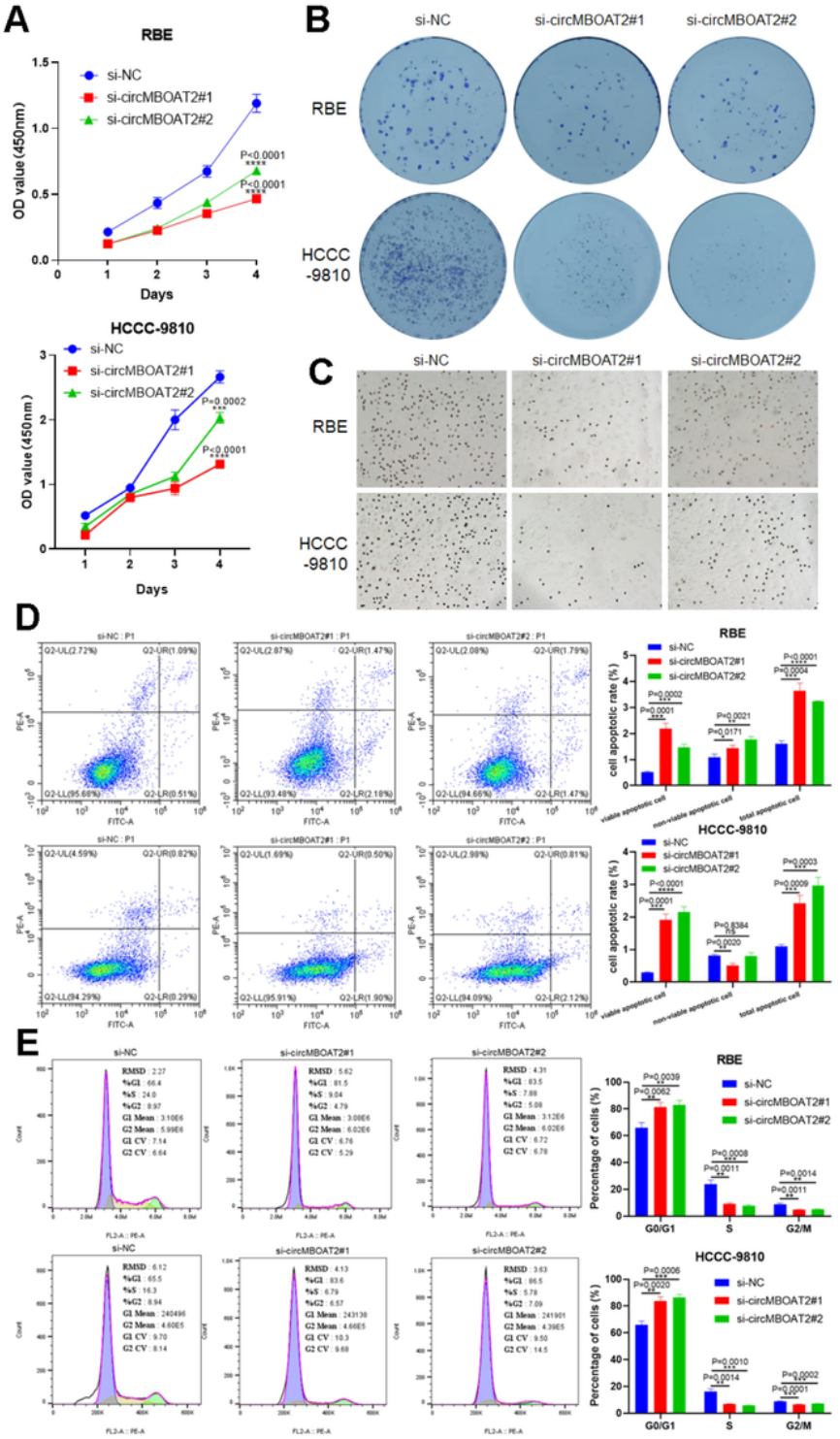

Figure 2

CircMBOAT2 promotes ICC progression in vitro. **a** CCK8 assay for cell proliferation capacity. The results showed that downregulation of circMBOAT2 inhibited the viability of RBE and HCCC-9810 cells. **b** Clone formation assay. The results showed that silencing circMBOAT2 inhibited the proliferative capacity of RBE and HCCC-9810 cells. **c** 5-Ethynyl-2'-deoxyuridine (EdU) proliferation assay. Knockdown of circMBOAT2 inhibits DNA synthesis in RBE and HCCC-9810 cells. The original magnification was 200×. **d** Data are expressed as the early and late stages of apoptosis rate after si-NC, si-circMBOAT2#1 or si-MBOAT2#2 transfection of RBE and HCCC-9810 cells. **e** The percentage cell phase distribution including G0/G1, S and G2/M phases after transfection of RBE and HCCC-9810 cells with si-NC, si-circMBOAT2#1 or si-MBOAT2#2.

Figure 3

CircMBOAT2 regulates lipid metabolism reprogramming especially unsaturated lipid. **a, b** The neutral lipid droplets were detected by staining with BODIPY 493/503 in RBE and HCCC-9810 cells transfected by si-NC, si-circMBOAT2#1 and si-MBOAT2#2. Nuclei were stained with DAPI. Scale bar = 50 μm. **c** The circMBOAT2 knockdown group was compared with the control group for GSEA analysis. Normalized enrichment score (NES)=1.232592. **d** Lipid species identified in lipidomics analysis, HCCC-9810 cells transfected with si-NC or si-circMBOAT2#1. FA fatty acids; Car carnitines; Cer ceramides; DG diradylglycerolipids; HexCer hexceramides; LPC lysophosphatidylcholines; LPE lysophosphatidylethanolamines; PC phosphatidylcholines; PE phosphatidylethanolamines; PG phosphatidylglycerols; PI phosphatidylinositols; PS phosphatidylserines; SM sphingomyelins; TG triradylglycerolipids. **e** HCCC-9810 cells were transfected with si-NC or si-circMBOAT2#1 for lipid principal component analysis (PCA). f Heat map of changes in lipid species.

Figure 4

CircMBOAT2 interacts with PTBP1 in ICC cells. **a** A RNA pull-down assay was performed; SDS-polyacrylamide gel electrophoresis (SDS/PAGE) and silver staining were used to detect RNA-related proteins. **b** Label-free intensity-based absolute quantification (iBAQ) method to quantify conjugated protein abundance with sense probe and anti-sense probe. **c** Western blot analysis was performed to detect the specific association of circMBOAT2 and PTBP1/FASN. β-actin was used as a negative control. **d, e** RNA immunoprecipitation (RIP) assay. CircMBOAT2 was precipitated by an anti-PTBP1 antibody specifically but an anti-FASN antibody nonspecifically then detected by qRT-PCR in HCCC-9810 cells. IgG was used as a negative control. **f** Immunofluorescence detected the co-localization of PTBP1 (green) with circMBOAT2 (red) in RBE and HCCC-9810 cells. Scale bar = 50 μm.

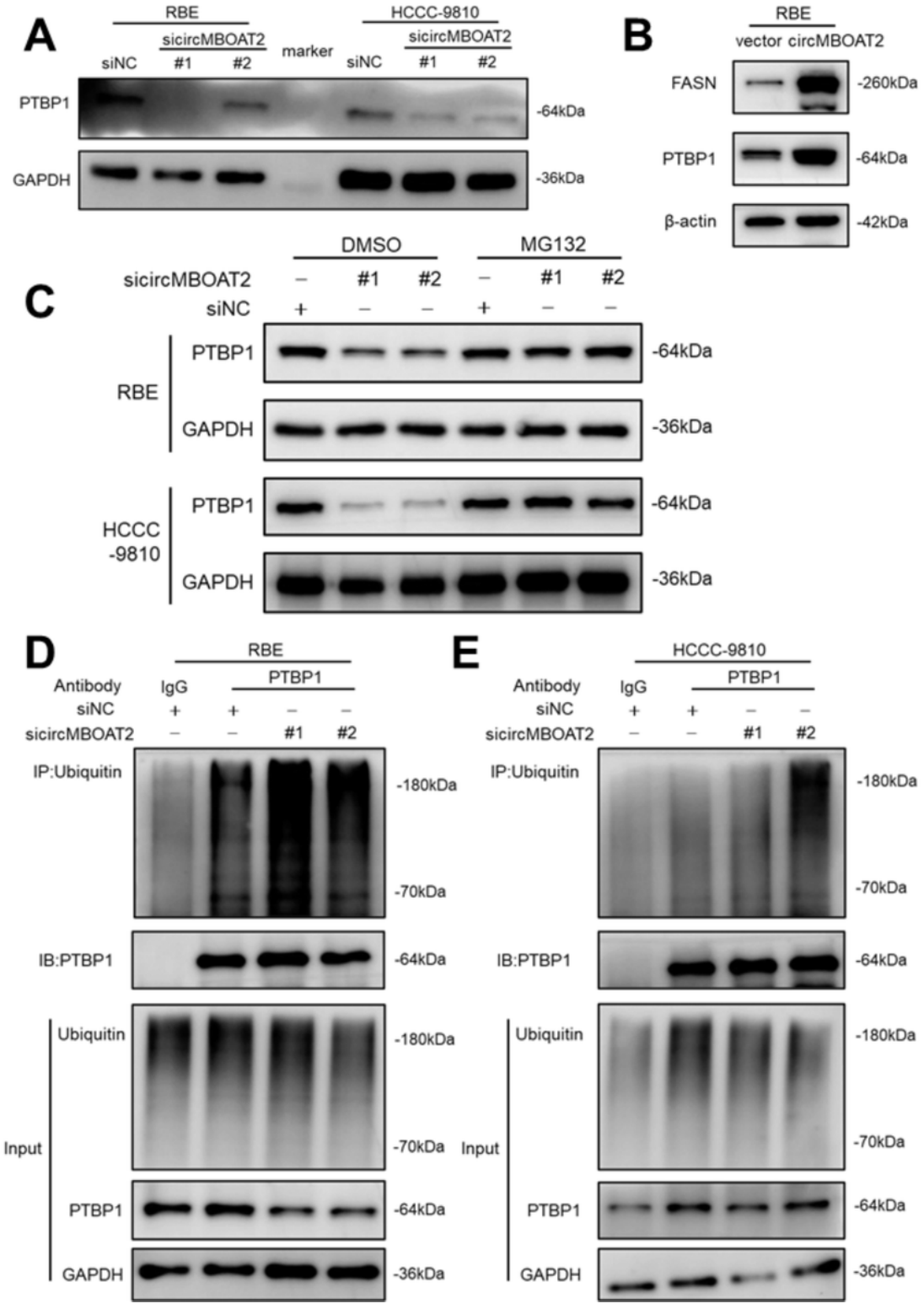

Figure 5

CircMBOAT2 protects PTBP1 from ubiquitin/proteasome-dependent degradation. **a** Protein levels of PTBP1 in RBE and HCCC-9810 cells with circMBOAT2 knockdown. GAPDH was used as a negative control. **b** Protein levels of PTBP1 and FASN in RBE cells with circMBOAT2 overexpression. **c** CircMBOAT2 knockdown and control RBE and HCCC-9810 cells were incubated with MG132 (10μM) for 8 hours.

Protein levels of PTBP1 were measured by western blot. **d, e** Immunoprecipitation detected ubiquitination modification of PTBP1 in RBE and HCCC-9810 cells. Ub ubiquitin.

Figure 6

CircMBOAT2 promotes PTBP1-mediated cytoplasmic export of FASN mRNA. **a** RIP assay. FASN mRNA was precipitated by an anti-PTBP1 antibody specifically, and detected by qRT-PCR in HCCC-9810 cells. IgG was used as a negative control. **b** The mRNA expression of FASN was determined with qRT-PCR, which was normalized to β-actin after transfection of RBE and HCCC-9810 cells with si-NC, si-PTBP1#1 or si-PTBP1#2. **c** Western blotting showed the protein levels of PTBP1 after transfection of RBE and HCCC-9810 cells with si-NC, si-PTBP1#1 or si-PTBP1#2. GAPDH was used as a negative control. **d** The qRT-PCR method was applied to detect the mRNA levels of FASN in 26 ICC patients and normal tissues adjacent to the cancer. The expression of FASN was normalized to β-actin. Significant differences between groups were analyzed by paired sample t-test. **e** The nuclear and cytoplasmic fractions were obtained by isolation. The qRT-PCR method was used to detect the mRNA levels of FASN in nuclear and cytoplasmic fractions of RBE and HCCC-9810 cells transfected with si-NC, si-PTBP1#1 or si-PTBP1#2. **f** The relative protein levels of PTBP1 and mRNA levels of FASN after transfected with si-NC, si-circMBOAT2#1 and si-MBOAT2#2 in HCCC-9810 cells were detected by immunofluorescence assays. Scale bar = 50 μm. **g** The protien levels of PTBP1 and FASN were determined by western blot analysis after PTBP1 knockdown and circMBOAT2 overexpression in RBE cells.

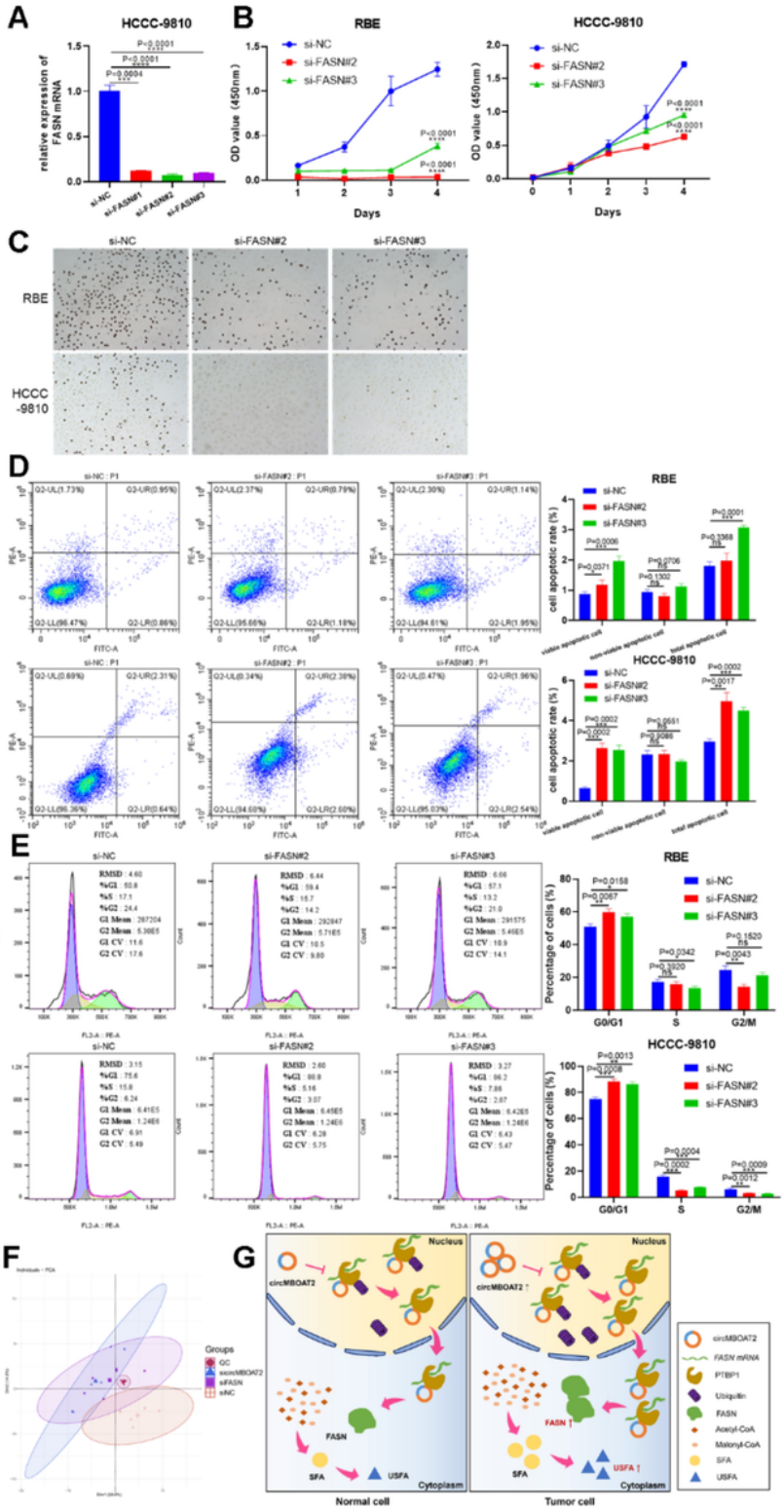

Figure 7

CircMBOAT2 promotes lipid metabolism reprogramming and progression in ICC through FASN. **a** The qRT-PCR method was applied to detect the mRNA levels of FASN after transfected with si-NC, si-FASN#1, si-FASN#2 and si-FASN#3. The expression of FASN was normalized to β-actin. **b** CCK8 assay for cell proliferation capacity after transfected with si-FASN#2 and si-FASN#3 in RBE and HCCC-9810 cells. **c** EdU proliferation assay was used to detect the levels of DNA synthesis in RBE and HCCC-9810 cells after

transfected to si-NC, si-FASN#2 and si-FASN#3. The original magnification was 200×. **d** Flow Cytometry was applied to determine the early and late stages of apoptosis rate after si-NC, si-FASN#2 and si-FASN#3 transfection of RBE and HCCC-9810 cells. **e** Flow Cytometry was applied to determine the percentage cell phase distribution including G0/G1, S and G2/M phases after transfection of RBE and HCCC-9810 cells with si-NC, si-FASN#2 and si-FASN#3. **f** HCCC-9810 cells were transfected with si-NC, si-circMBOAT2#1 or si-FASN#2 for lipid principal component analysis (PCA). **g** Illustration of the mechanism of circMBOAT2 on promoting CRC progression via circMBOAT2/PTBP1/FASN signaling pathway.

Supplementary Files

This is a list of supplementary files associated with this preprint. Click to download.

- Additionalfile1.SupplementaryMaterials.doc
- Additionalfile2.SupplementaryFigures.doc
- Additionalfile3.SupplementaryTable1.xls
- Additionalfile4.SupplementaryTable2.xlsx
- Additionalfile5.SupplementaryTable3.xlsx
- Additionalfile6.SupplementaryTable4.xlsx